A&A manuscript no.
(will be inserted by hand later)

Your thesaurus codes are:
11.08.1; 11.09.4; 11.17.1; 11.17.4 Q1026-0045A,B

ASTRONOMY AND ASTROPHYSICS

HST observations of the QSO pair Q1026–0045A,B ⋆

Patrick Petitjean[1,2], Jean Surdej[3,7], Alain Smette[4], Peter Shaver[5], Jan Mücket[6], and Marc Remy[3]

[1]Institut d'Astrophysique de Paris - CNRS, 98bis Boulevard Arago, F-75014 Paris, France
[2]UA CNRS 173- DAEC, Observatoire de Paris-Meudon, F-92195 Meudon Principal Cedex, France
[3] Institut d'Astrophysique, Université de Liège, Avenue de Cointe 5, B–4000 Liège, Belgium
[4] NASA-Goddard Space Flight Center, Code 681, Greenbelt, MD 20771, USA
[5] European Southern Observatory, Karl−Schwarzshild−Str. 2, D-80547 Garching bei München, Germany
[6]Astrophysikalisches Institut Potsdam, An der Sternwarte 16, D-14482 Potsdam, Germany
[7] Directeur de Recherches du FNRS, Belgium

Abstract. The spatial distribution of the Lyα forest is studied using new HST data of the quasar pair Q 1026–0045 A and B at $z_{\rm em}$ = 1.438 and 1.520 respectively. The angular separation is 36 arcsec and corresponds to transverse linear separations between lines of sight of $\sim$300h_{50}^{-1} kpc ($q_{\rm o}$ = 0.5) over the redshift range $0.833 < z < 1.438$. From the observed numbers of coincident and anti-coincident Lyα absorption lines, we conclude that, at this redshift, the Lyα structures have typical dimensions of $\sim$500h_{50}^{-1} kpc, larger than the mean separation of the two lines of sight. The velocity difference, ΔV, between coincident lines is surprisingly small (4 and 8 pairs with $\Delta V < 50$ and 200 km s^{-1} respectively).
Metal line systems are present at $z_{\rm abs}$ = 1.2651 and 1.2969 in A, $z_{\rm abs}$ = 0.6320, 0.7090, 1.2651 and 1.4844 in B. In addition we tentatively identify a weak Mg II system at $z_{\rm abs}$ = 0.11 in B. It is remarkable that the $z_{\rm abs}$ = 1.2651 system is common to both lines of sight. The system at $z_{\rm abs}$ = 1.4844 has strong O VI absorption.
There is a metal-poor associated system at $z_{\rm abs}$ = 1.4420 along the line of sight to A with complex velocity profile. We detect a strong Lyα absorption along the line of sight to B redshifted by only 300 km s^{-1} relatively to the associated system. It is tempting to interpret this as the presence of a disk of radius larger than 300h_{50}^{-1} kpc surrounding quasar A.

Key words: quasars:individual:Q 1026–0045A,B, Galaxies: ISM, quasars:absorption lines, Galaxies: halo

1. Introduction

One way to probe the transverse extension of the gaseous structures giving rise to the Lyα forest seen in the spectrum of quasars is to observe multiple lines of sight to quasars with small angular separations on the sky and search the spectra for absorptions coincident in redshift.

This technique originated with a suggestion by Oort (1981) to test the possibility that the Lyα forest clouds originate in large pancake structures. This proposal was contradicted by Sargent et al. (1982) who found no tendency for Lyα lines to correlate in the spectra of Q1623+269 and Q1623+268 separated by 2.9 arcmin on the sky. The first discoveries of common and associated absorptions in the spectra of pairs of distinct quasars with separations of the order of one arcmin, made by Shaver, Boksenberg & Robertson (1982) and Shaver & Robertson (1983), indicated however the possible existence of very large absorber sizes (hundreds of kpc), even for the Lyα clouds. Spectra of pairs of gravitational lens images also revealed common absorptions on smaller scales (Weyman & Foltz 1983, Foltz et al. 1984). Years later, the large sizes of absorbers were confirmed by Smette et al. (1992), Dinshaw et al. (1994), Bechtold et al. (1994), Crotts et al. (1994), Bechtold & Yee (1994), Smette et al. (1995), D'Odorico et al. (1998).

Recently, Dinshaw et al. (1995) derived a radius of 330h_{50}^{-1} kpc at $z \sim 0.7$ for spherical clouds from observation of Q0107–0232 and Q0107–0235 separated by 86 arcsec. Larger separations have been investigated by Crotts & Fang (1997) and Williger et al. (1997). Both studies conclude that the clouds should be correlated on scales larger than 500 kpc.
Here we present observations of Q1026–005 A ($m_{\rm r}$ = 18.4, $z_{\rm em}$ = 1.438) and B ($m_{\rm r}$ = 18.5, $z_{\rm em}$ = 1.520), two distinct quasars separated on the sky by 36 arcsec or 300 h_{50}^{-1} kpc ($q_{\rm o}$ = 0.5) at $z \sim 1$.

2. Observations

The observations were carried out on the Hubble Space Telescope using the Faint Object Spectrograph with the G270H grating over the wavelength range 2250–3250 Å, for a resolution of 1.92 Å FWHM. A total of 5300 s integration time was accumulated on both quasars. The data were calibrated using the standard pipeline reduction techniques. The zero point

Send offprint requests to: P. Petitjean

⋆ Based on observations obtained with the NASA/ESA *Hubble Space Telescope* by the Space Telescope Institute, which is operated by AURA, Inc., under NASA contract NAS 5-26555

Table 1. Line list

Q1026-0045A $\lambda_{\rm obs}$ (Å)	$w_{\rm obs}$ (Å)	S/N	Ident.	z	Q1026-0045B $\lambda_{\rm obs}$ (Å)	$w_{\rm obs}$ (Å)	S/N	Ident.	z	[a]
		7			2229.2:	0.6:	7	SiII1304	0.7090	
2233.76	1.53	8	Lyγ	1.2968			12			
2244.20	1.10	8	CIII977	1.2970			12			
2259.87	0.51	11	Lyα	0.8589		<0.45	12			u/u/u
2273.23	0.55	9	NIII989	1.2967			12			
	<0.60	9			2274.68	0.67	12	SiIV1393	0.6320	
		8			2281.17	2.19	12	CII1334	0.7093	
	<0.65	8			2288.50	0.9:	12	Lyα	0.8825	u/u/u
								SiIV1402	0.6320	
		14			2312.30	0.49	14	Ly6	1.4843	
2319.2:	0.35	14	Lyδ	1.4419			14			
2323.54	1.28	13	Lyβ	1.2653	2323.65	0.73	14	Lyβ	1.2654	
	<0.40	13			2330.03	1.22	15	Lyα	0.9166	u/u/u
								Lyϵ	1.4846	
2338.16	1.32	10	Lyβ	1.2802	2337.93	0.50	15	Lyα	0.9231	u/u/u
		14			2344.34	0.50	15	FeII2344	0.0000	
2355.48	1.95	10	Lyβ	1.2964			15			
		10			2359.85	0.96	15	Lyδ	1.4847	
2368.92	1.28	11	Lyα	0.9486	2368.97	1.19	14	Lyα	0.9486	C/C/C
2375.03	2.08	11	Lyγ	1.4405	2376.05	1.51	14	Lyγ	1.4438	
			Lyγ	1.4419				FeII2344	0.0000	
			Lyα	0.9536				Lyα	0.9545	u/u/u
2380.26	0.77	11	CII1036	1.2968						
2382.97	0.90	11	FeII2382	0.0000	2382.25	1.52	15	FeII2382	0.0000	
								SiIV1393	0.7092	
2392.90	1.13	11	Lyα	0.9683		<0.38	14			u/A/u
		11			2397.06	0.56	14	SiIV1402	0.7088	
		11			2415.90	1.00	14	Lyγ	1.4841	
	<0.45	11			2419.8:	0.32	15	Lyα	0.9904	u/u/u
	<0.45	11			2424.53	0.42	15	Lyα	0.9943	u/u/u
		11			2427.30	0.65	17	CIII977	1.4844	
	<0.45	11			2444.15	0.85	19	Lyα	1.0105	u/A/u
2450.0:	0.75	12	Lyα	1.0153		<0.28	19			u/u/u
2454.0:	0.34	15	Lyα	1.0186	2454.32	0.63	19	Lyα	1.0189	A/A/u
2458.47	0.61	15	Lyα	1.0223	2458.65	0.30	19	NIII989	1.4840	A/A/u
2474.3:	0.25	15	Lyα	1.0353	2475.8	0.35	19	Lyα	1.0365	u/u/u
		15			2491.71	0.83	19	SiII1526	0.6321	
2497.51	1.29	15	Lyα	1.0544	2497.24	0.49	19	Lyα	1.0542	C/A/A
2503.30	1.30	14	Lyβ	1.4405			19			
2504.66	1.20	14	Lyβ	1.4419	2506.65	0.59	19	Lyβ	1.4438	
		12			2521.88	0.26	21	Lyα:	1.0744	u/u/u
	<0.38	12			2526.44	1.52	21	Lyα	1.0782	A/u/u
								CIV1548	0.6321	
		12			2531.03	0.46	21	CIV1550	0.6321	
		12			2548.25	1.22	21	Lyβ	1.4844	
		12			2563.70	0.84	21	OVI1031	1.4844	
2568.5:	0.38	14	Lyα	1.1128		<0.28	19			u/u/u

Q1026-0045A $\lambda_{\rm obs}$ (Å)	$w_{\rm obs}$ (Å)	S/N	Ident.	z	Q1026-0045B $\lambda_{\rm obs}$ (Å)	$w_{\rm obs}$ (Å)	S/N	Ident.	z	[a]
2575.22	1.70	15	Lyα	1.1183	2575.37	0.82	19	Lyα	1.1184	C/C/A
		15			2577.5:	0.59	19	OVI1037	1.4841	
2586.35	0.50	15	FeII2586	0.0000	2587.9:	0.42	15	FeII2586	0.0000	
2600.58	1.40	15	FeII2600	0.0000	2601.2:	1.23	19	FeII2600	0.0000	
		16			2608.74	0.79	19	SiII1526	0.7087	
		16			2625.28	0.51	20	FeII1608	0.6322	
		13			2645.44	0.83	18	CIV1548	0.7087	
		13.0			2650.08	0.67	18	CIV1550	0.7089	
	<0.35	13			2669.58	0.42	18	Lyα	1.1959	u/u/u
		13			2726.96	0.90	18	AlII1670	0.6321	
2733.15	1.06	14	SiII1190	1.2968			18			
			SiIII1206	1.2650						
2736.63	0.52	14	Lyα	1.2511		<0.25	21			A/u/u
2740.75	0.87	14	SiII1193	1.2968			21			
	<0.32	14			2745.29	0.75	20	Lyα	1.2582	A/A/u
		14			2748.47	0.63	20	FeII1608	0.7088	
2753.67	2.42	14	Lyα	1.2651	2753.74	1.50	20	Lyα	1.2651	M_c
2772.06	3.10	14	SiIII1206	1.2976			15			
			Lyα	1.2802						A/A/A
2792.35	6.62	14	Lyα	1.2969		<0.36	15			M_a
2796.05	2.20	14	MgII2796	0.0000	2796.90:	1.95	15	MgII2796	0.0000	
2803.60	1.17	14	MgII2803	0.0000	2803.54	0.98	15	MgII2803	0.0000	
2807.94	0.44	14	Lyα	1.3097		<0.36	15			u/u/u
2820.08	0.73	14	Lyα	1.3197	2819.87	0.74	17	Lyα	1.3195	C/C/u
2849.12	0.80	14	Lyα	1.3436		<0.24	22			A/A/u
		14			2854.78	1.10	20	AlII1670	0.7086	
2895.00	1.85	15	SiII1260	1.2969			16			
2961.76	0.28	20	Lyα	1.4363						
2966.45	0.97	20	Lyα	1.4401			23			
2968.69	1.42	20	Lyα	1.4420	2971.09	1.30	18	Lyα	1.4439	
2991.08	0.30	18	OI1302	1.2970			16			
2995.36	0.66	18	SiII1304	1.2964			16			
		18			2997.47	0.66	16	SiIII1206	1.4844	
		18			3008.06	0.40	16	Lyα	1.4743	
								AlIII1854:	0.6219	
		18			3020.05	1.75	16	Lyα	1.4842	
		18			3027.51:	0.53	16	AlIII1862:	0.6252	
3065.05	0.86	16	CII1334	1.2967			18			
		13			3104.81	0.36	20	MgII2796	0.1103	
		13			3113.13	0.30	22	MgII2803	0.1104	
								CIV1548?	1.0106	
		13			3118.00	0.20:	22	CIV1550?	1.0106	
3156.92	0.32	15	SiIV1393	1.2650	3155.87	0.57	16	SiIV1393?	1.2643	
		15			3168.43	0.44	16	AlIII1854?	0.7083	
3177.14	0.24	15	SiIV1402	1.2649			16			
3201.42	0.62	12	SiIV1393	1.2970			16			
3222.51	0.54	12	SiIV1402	1.2972			18			

[a] Correlations are marked by a "C", anti-correlation by a "A" and ambiguous cases by a "u" for $w_{\rm r} > 0.2$,0.3 and 0.6 Å.
* A colon means uncertain value or identification

of the wavelength scale was determined requiring that Galactic interstellar absorptions occur at rest. The spectra are shown in Fig. 1, the line–lists are given in Table 1.

3. Results

3.1. The metal line systems

Metal line systems are present at $z_{\rm abs}$ = 1.2651 and 1.2969 in A, $z_{\rm abs}$ = 0.11, 0.6320, 0.7090, 1.2651 and 1.4844 in B.

In A, the system at $z_{\rm abs}$ = 1.2651 is detected by strong H I$\lambda\lambda$1025,1215 absorptions and has a Si IV$\lambda\lambda$1393,1402 doublet associated. There are strong H I$\lambda\lambda$1025,1215 absorptions at the same redshift along the line of sight to B. The fact that the positions of the H I absorptions in A and B are nearly identical (λ2753.67 and λ2753.74 Å for Lyα respectively) argues for the two absorptions beeing produced by the same object. If true the transverse dimension is larger than the 310 h_{50}^{-1}kpc separation between the two lines of sight. The system at $z_{\rm abs}$ = 1.2969 has strong H I ($w_{\rm r}$(Lyα) = 2.9 Å) C II, C III, O I, N III, Si II, Si III, Si IV absorptions.

In B, both $z_{\rm abs}$ = 0.6320 and 0.7090 systems have strong Si IIλ1526, Fe IIλ1608, Al IIλ1670 and C IVλ1550 absorptions. As said before the $z_{\rm abs}$ = 1.2651 system is common to A and B. The presence of metals is revealed only by a λ3155.87 feature that we identify as Si IVλ1393. The associated Si IVλ 1402 line is not detected but could be lost in the noise. The strong system at $z_{\rm abs}$ = 1.4842 shows N III, C III, Si III and possibly O VI associated absorptions. O VI absorption seems to be detected in most of the low and intermediate redshift systems (Bergeron et al. 1994, Vogel & Reimers 1995, Burles & Tytler 1996) and has been observed in a few high redshift Lyman limit systems (Kirkman & Tytler 1997). Although the velocity difference with the quasar is larger than 4000 km s^{-1}, there is a possiblility that the system is associated with the quasar. In addition we tentatively identify a weak ($w_{\rm r} \sim 0.3$Å) Mg II system at $z_{\rm abs}$ = 0.11 in B. Mg IIλ2803 is possibly blended with C IVλ1548 of a possible weak C IV system at $z_{\rm abs}$ = 1.0106.

3.2. The associated system in A and the proximity effect

There is a strong associated system detected in A by its H I Lyα and Lyβ absorptions. Two components are seen at $z_{\rm abs}$ = 1.4401

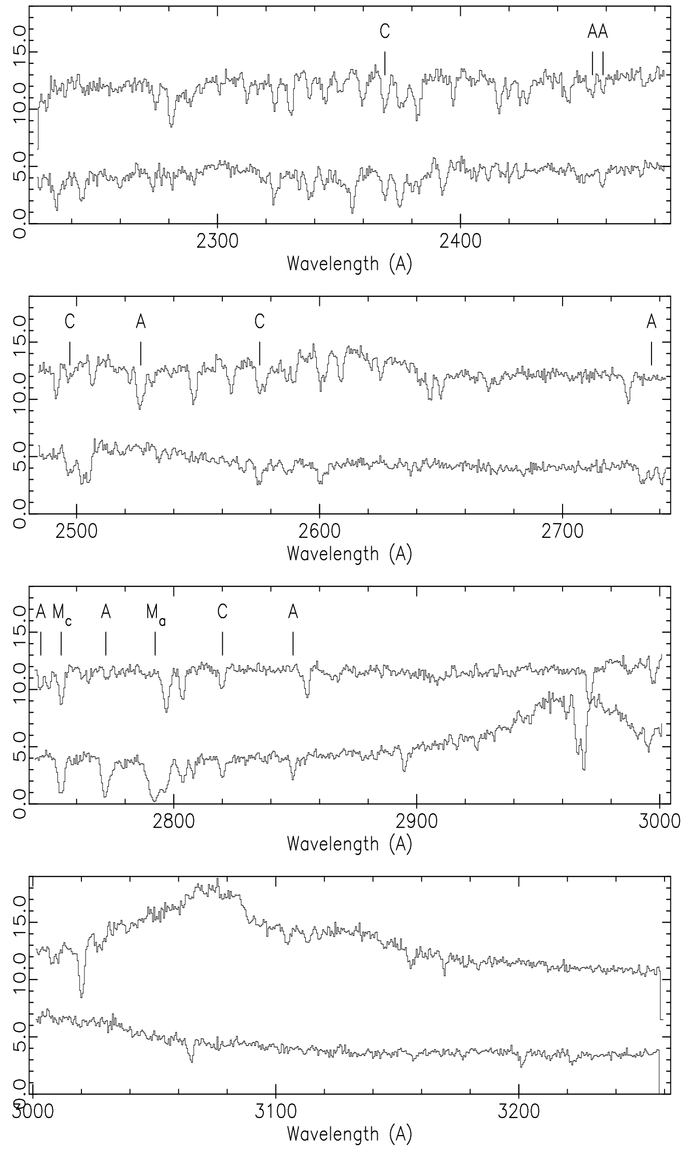

Fig. 1. Spectra of Q1026–0045 A (bottom line) and B (top line). Flux is given in units of 10^{-16} erg/s/cm^{-2}/Å. The spectrum of B has been shifted by 6.5 in the same units. A and C marks indicate anti-correlation and correlation for Lyα forest lines with $w_{\rm r} > 0.2$ Å. $\rm M_a$ and $\rm M_c$ marks have the same signification for Lyα lines from metal line systems.

and 1.4420 with $w_{\rm r}$(Lyα) = 0.58 and 0.40 Å respectively. The two components are *redshifted* relative to the QSO by 260 and 490 km s^{-1}. Since the true redshift of the quasar is poorly known, these values are very uncertain. We do not detect any metal lines in the system. The O VI lines have $w_{\rm r} < 0.20$ Å; the C IV lines are redshifted outside the wavelength range of the data. Interestingly enough, there is a H I absorption system at $z_{\rm abs}$ = 1.4439 along the line of sight to Q 1026–0045B. The velocity difference between this system and the $z_{\rm abs}$ = 1.4420 in A is about 230 km s^{-1} only.

It is unlikely that the $z_{\rm abs} \sim z_{\rm em}$ system is intrinsically associated with the central AGN. Such systems usually have high metal content and are expected to exhibit strong O VI and N V absorptions (Petitjean et al. 1994, Hamann 1997), absent from the spectra of Q1026–0045 A & B. The three absorptions are thus part of an object or group of objects which transversal dimension exceeds the $300h_{50}^{-1}$ kpc separation between the two lines of sight.

The absence of metals in the system associated with A, over the observed wavelength range, suggests an intergalactic origin. The higher velocity of the gas along the line of sight to B argues against the simple picture in which the gas would be collapsing toward A. In that case, we would expect the gas along the line of sight to B to have a projected velocity smaller than the velocity of the gas just in front of A. A model where the gas would be part of a rotating disk can be accomodated if the component at z = 1.4420 is at the same redshift as the quasar. In this case however one could wonder why the gas is metal deficient.

The relative equivalent widths of the hydrogen lines in the Lyman series of the system at $z_{\rm abs}$ = 1.4842 toward B are indicative of H I column densities in excess of 10^{16} cm^{-2}. The presence of strong metal lines suggests that the gas is associated with the halo of a galaxy. Very deep imaging in this field to search for any enhanced density of objects would help to understand the nature of these intriguing systems.

There are only two systems in both lines of sight from z = 1.3436 to 1.520, the associated system in A (and its counterpart in B) and the metal system at z = 1.4842 in B. The number of lines with $w_{\rm r} > 0.24$ Å expected in this redshift range is 7±2 (Bahcall et al. 1996). The random probability to detect zero line when seven are expected is $9.1^{67}_{1.2}\times 10^{-4}$. It is probable that we see the effect of the enhanced photo-ionizing field due to the proximity of the quasars.

3.3. *The Lyα forest*

3.3.1. The line-lists

Table 1 lists all the absorption features detected at the 3σ level in the spectra. Identification of Lyα lines is sometimes uncertain due to blending with lines from the numerous metal line systems. We discuss here individual lines.

In Q 1026–0045A, the λ2259 feature could be partly Lyϵ from the $z_{\rm abs}$ = 1.4420 system but given the strength of the other lines in the series, the contribution is most certainly negligible. There is a broad feature centered at 2452 Å that we decompose into two components at 2450 and 2454 Å. This feature is uncertain however. Galactic Fe IIλ2374 absorption should not contribute to much to the λ2375 feature that is mostly Lyγ at $z_{\rm abs}$ = 1.4405 and 1.4420. The line is quite strong however and could be produced partly by a Lyα absorption at $z_{\rm abs}$ = 0.9536. The two lines at λ2458 and λ2474 could correspond to a Si IVλ λ1393,1402 doublet at $z_{\rm abs}$ = 0.7639. The corresponding C IIλ 1334 line would be blended with Lyβ at $z_{\rm abs}$ = 1.2964 but the

feature at λ2736 could be C IVλ1550 at the same redshift with no C IVλ1548 detected. The line however is displaced by more than 1 Å from the expected position which is not acceptable. We thus consider the Si IV identification as doubtful.
In Q 1026–0045B, there is a broad feature at λ2288.5 that cannot be accounted for by Si IVλ1402 at z = 0.6320 only. The feature at λ2376 may have a double structure. Lyγ at 1.4438 and Fe IIλ2374 definitively contribute to this feature which is strong enough however to be partly produced by Lyα absorption at $z_{\rm abs}$ = 0.9545. Since C IVλ1550 at $z_{\rm abs}$ = 0.6321 has $w_{\rm obs}$ = 0.46 Å, C IVλ1548 at the same redshift should have $w_{\rm obs}$ < 0.92 Å. Consequently there is a Lyα line at $z_{\rm abs}$ = 1.0782 with $w_{\rm obs} > 0.6$ Å.

We detect 11 and 12 Lyα lines with $w_{\rm r} > 0.2$ Å over the redshift range 0.8335–1.3436 along the lines of sight to A and B respectively. The density of lines with $w_{\rm r} > 0.24$ Å detected by the HST in the same redshift range is $\sim$36$\pm$10 (Jannuzi et al. 1998). The number of lines we detect is thus small. This might be a consequence of blending effects. Last column of Table 1 indicates for each Lyα line with $w_{\rm r} >$ 0.2, 0.3, 0.6 Å whether there is correlation (C) or anti-correlation (A). A letter (u) marks lines that are out of the sample or uncertain cases because of blending effets. A symbol (M) indicates Lyα lines from metal line systems.

3.3.2. Correlations

The numbers of coincidences and anticoincidences for $w_{\rm r} > 0.2$, 0.3 and 0.6 Å are 4, 3, 1 and 7, 8, 3 respectively. Assuming that the Lyα clouds are spheres of radius R, we calculate the density probability for R (see Fig. 2) following Fang et al. (1996). The peak of the probability is at R = 267, 305 and 364h_{50}^{-1} kpc for $w_{\rm r} >$ 0.6, 0.3 and 0.2 Å. There is a hint for the dimensions of the structures to be larger for smaller equivalent widths. This property is expected in simulations (Charlton et al. 1997). However as shown by Fang et al. (1996) and Crotts & Fang (1997), the radius determined by this method increases with the separation of the lines of sight indicating that the assumption of a single structure size is invalid. This has been recognized to be a characteristic of the spatial distribution of the Lyα gas in the simulations (Charlton et al. 1997). It is clear that better statistics in the data are needed to have a better understanding of the structures especially to discuss the difference between real size of the clouds and correlation length (Cen & Simcoe 1997).

It is intriguing to note that the velocity difference ΔV between lines coincident in redshift in the two lines of sight is small. Considering all the pairs, we find 4 and 8 pairs with $\Delta V <$ 50 and 200 km s^{-1} respectively. There is no pair, even along one single line of sight with 200 $< \Delta V <$ 400 km s^{-1}. This has been shown to favor disk-like structures (Charlton et al. 1995) but should be studied in more detail.

Acknowledgements. MR and JS wish to thank the SSTC/PRODEX project for partial support during this work.

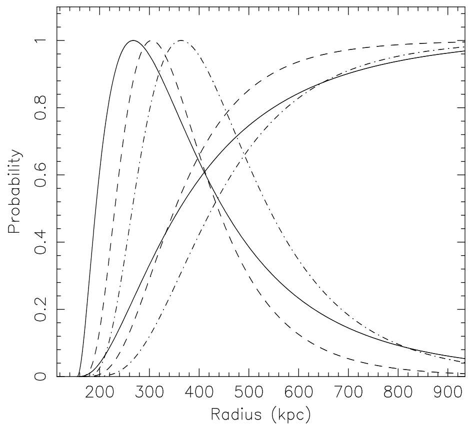

Fig. 2. Probability distribution $P(R)$, normalized to one at its peak, and cumulative distribution versus cloud radius from the number of coincidences and anticoincidences of Lyα lines with $w_{\rm r} > 0.2$ (dashed-dotted lines), 0.3 (dashed lines) and 0.6 Å(solid lines). The peak of the probability is at R = 267, 305 and 364h_{50}^{-1} kpc for $w_{\rm r} >$ 0.6, 0.3 and 0.2 Å respectively.

References

Bahcall J.N., Bergeron J., Boksenberg A., et al., 1996, ApJ 457, 19
Bechtold J., Crotts A.P.S., Duncan R.C., Fang Y., 1994, ApJ 437, L83
Bechtold J., Yee H.K.C., 1994, AJ 110, 1984
Bergeron J., Petitjean P., Sargent W.L.W., et al., 1994, ApJ 436, 33
Burles S., Tytler D., 1996, ApJ 460, 584
Cen R., Simcoe R.A., 1997, ApJ 483, 8
Charlton J.C., Anninos P., Zhang Y., Norman M.L., 1997, ApJ 485, 26
Charlton J.C., Churchill C.W., Linder S.M., 1995, ApJ 452, L81
Crotts A.P.S., Bechtold J., Fang Y., Duncan C., 1994, ApJ 437, 79
Crotts A.P.S., Fang Y., 1997, astro-ph 9702185
Dinshaw N., Foltz C.B., Impey C.D., Weymann R.J., Morris S.L., 1995, Nature 373, 223
Dinshaw N., Impey C.D., Foltz C.B., Weymann R.J., Chaffee F.H.Jr., 1994, ApJ 437, L87
D'Odorico S., Cristiani S., D'Odorico V., et al., 1998, in P. Petitjean & S. Charlot, XIII^e IAP Colloquium, Editions Frontières, Paris, in press
Fang Y., Duncan R.C., Crotts A.P.S., Bechtold J., 1996, ApJ 462, 77
Foltz C.B., Weymann R.J., Röser H.J., Chaffee F.H.Jr., 1984, ApJ 281, L1
Hamann F., 1997, ApJS 109, 279
Jannuzi B., et al., 1998, ApJS in press
Kirkman D., Tytler D., 1997, ApJ 489, L123
Oort J.H., 1981, A&A, 94, 359
Petitjean P., Rauch M., Carswell R.F., 1994, A&A 291, 29
Sargent L.W.L., Young P., Schneider D.P., 1982, ApJ 256, 374
Shaver P.A., Boksenberg A., Robertson J.G., 1982, ApJ 261, L7
Shaver P.A., Robertson J.G., 1983, ApJ 268, L57
Smette A., Robertson J.G., Shaver P.A., et al., 1995, A&AS 113, 199
Smette A., Surdej J., Shaver P.A., et al., 1992, A&A 389, 39
Vogel S., Reimers D., 1995, A&A 294, 377
Weymann R.J., Foltz C.B., 1983, ApJ 272, L1
Williger G.M., Smette A., Hazard C., Baldwin J.A., McMahon R.G., 1997, astro-ph/9709170